Oxaaza cyclophanes in the recognition of nucleotides. The role of oxygen and electron-rich aromatic rings†

M. I. Burguete,[a] E. García-España,[b] L. López-Diago,[a] S. V. Luis,[a] J. Miravet[a] and D. Sroczynski[a]

Received 21st March 2007, Accepted 26th April 2007
First published as an Advance Article on the web 15th May 2007
DOI: 10.1039/b704305h

Dioxapolyaza cyclophanes derived from resorcinol and different polyamine chains have been studied in aqueous solution as abiotic receptors for nucleotides. The presence of the additional ethyleneoxy subunits is reflected in a higher basicity and in a significant increase in the log *K* values for the interaction with nucleotides relative to that of related polyazacyclophanes.

Introduction

Recognition of nucleotides is an essential event in many biological processes. Accordingly, a great deal of experimental effort has been addressed to designing abiotic selective receptors for nucleotides in order to establish the molecular basis of such events.[1–3] Nucleotide recognition needs to take into account the existence of different structural components: the purine or pyrimidine base, the sugar fragment and the phosphate terminal chain (Fig. 1). Although in aqueous solutions, charge–charge interactions between the anionic phosphate chain and oppositely charged receptors will represent the main contribution to the binding, other interactions like hydrogen-bonding between complementary hydrogen bond donor–acceptors of the nucleotide and the receptor as well as π–π and solvophobic interactions can also contribute significantly and modulate the selectivity patterns.[4] In this respect, we have recently prepared a series of receptors in which a resorcinol-derived aromatic fragment is linked to different polyamine chains (Fig. 1).[5] The charge–charge contribution will be provided by the interaction of the protonated polyamine fragment with the phosphate chain while the electron rich aromatic fragment can give rise to π–π interactions with the electron poor aromatic rings of the protonated nucleobases. The oxygen atoms can eventually contribute to the binding as hydrogen acceptors, while the protonated nitrogen atoms of the base or the hydroxyl groups of the sugar act as the donors.

Results and discussion

Acid–base properties

Compounds **Re33**, **Re222**, **Re323** and **Re343** (see Chart 1) were efficiently prepared according to a synthetic procedure we have previously reported.[4]

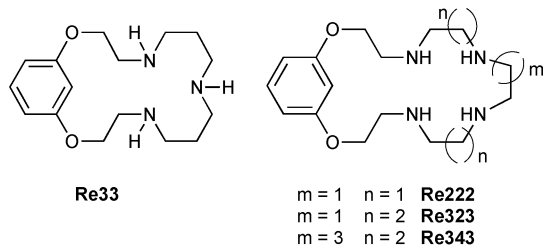

Chart 1

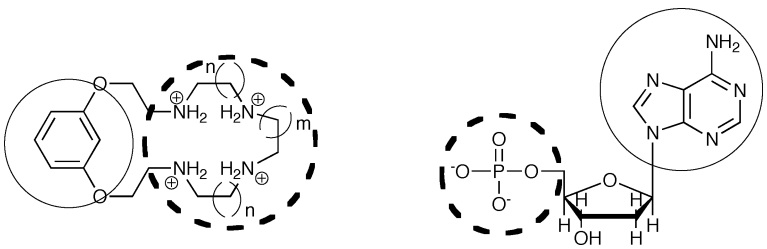

Fig. 1 Structural components of receptors: the purine or pyrimidine base, the sugar fragment and the phosphate terminal chain

[a]*Department of Inorganic and Organic Chemistry, UAMOA. University Jaume I/CSIC, E-12071, Castellón, Spain. E-mail: luiss@qio.uji.es; Fax: +34 964728214; Tel: +34 964728239*
[b]*Department of Inorganic Chemistry, Instituto de Ciencia Molecular, University of Valencia, P.O. Box 22085, 46071, Valencia. E-mail: Enrique.Garcia-España@uv.es*

† Electronic supplementary information (ESI) available: NMR titrations, distribution diagrams, suggested protonation sequences, calculated minimum energy structures for the ligands and their complexes. See DOI: 10.1039/b704305h

Table 1 Logarithms of the successive protonation constants for compounds in Chart 1 measured potentiometrically at 298.1 K in NaCl 0.15 mol dm^{-3}

Reaction[a]	**Re33**	**B33**[c]	**Re222**	**B222**[c]	**Re323**	**B323**[c]	**Re343**	**B343**[c]
$H + L = HL$	10.0(8)[b]	10.13(1)	10.21(2)	9.39(2)	10.12(1)	9.93(1)	10.84(2)	10.39(2)
$H + HL = H_2L$	8.29(1)	8.34(1)	8.75(2)	8.45(2)	9.09(1)	9.09(1)	9.82(1)	9.54(2)
$H + H_2L = H_3L$	6.74(1)	6.82(3)	7.66(3)	5.38(2)	7.44(1)	7.44(1)	7.73(2)	7.54(2)
$H + H_3L = H_4L$			3.09(4)	2.51(1)	5.03(2)	3.61(1)	6.87(2)	6.64(2)
$nH + L = H_nL$	25.33	25.29	29.72	25.73	31.67	30.07	35.26	34.11

[a] Charges omitted for clarity. [b] Standard deviations given in parenthesis. [c] See ref. 5.

In the work with polyamine ligands, an appropriate study of the acid–base properties is essential. The previous determination of their protonation constants is required in order to obtain the corresponding constants for the interaction of those receptors with different guests in aqueous media. On the other hand, the knowledge of the protonation degrees and that of the nature of the protonated species at the pH values of interest is essential in order to understand and rationalize their coordinating ability towards either cationic substrates or anionic species such as nucleotides.

Potentiometric measurements

In our case, protonation constants for macrocycles **Re33**, **Re222**, **Re323** and **Re343** were obtained by potentiometric measurements. The methodology used and the experimental set-up have been described in detail elsewhere.[6] All potentiometric measurements were carried out at 298.1 K. Table 1 gathers the successive stability constants calculated for the protonation of those macrocyclic compounds. For comparison, the corresponding constants for related polyazacyclophanes previously studied by our group and containing the same polyamine chains have also been included.[6]

As can be seen in the table, all the ligands show a significant decrease in the values of the successive protonation constants as the protonation degree increases. This is always the expected trend resulting from the electrostatic repulsions originated when a new proton is added to a previously protonated (charged) species. For the larger macrocycles (**Re343** and **Re323**), the difference between the first and the second protonation constants is small ($\Delta\log K = 1.02$ and 1.03 respectively) showing that those large macrocycles are able to accommodate two protons without paying any significant cost in terms of electrostatic repulsions. $\Delta\log K$ values are slightly higher for the smaller macrocycles. In general, it is to be expected that, for this kind of polyazamacrocycles, introduction of the third proton is accompanied by a more significant decrease of the values for the respective stability constants.[6,7] This is particularly relevant for the relatively small macrocycle **B222**, for which the third protonation needs to occur adjacent to one protonated nitrogen separated through a short ethylenic spacer. Such a drastic decrease is not observed, however, for receptor **Re222** that shows a log K value for this step two orders of magnitude higher than that measured for **B222**. The fourth protonation step shows, for the three tetraazamacrocycles (**Re222**, **Re323**, **Re343**), a log K value much lower than that for the formation of H_3**L**. This occurs as H_4**L** requires location of the incoming proton between two adjacent protonated (charged) nitrogen atoms. Nevertheless, the decrease observed for **Re323** is again less marked than that for **B323** giving place to a fourth log K value significantly higher for **Re323**.

According to the former considerations, except for the smallest macrocycle of the series, the overall basicity of the new macrocycles is higher than that of the corresponding polyazacyclophanes, in particular for the **Re222** (four orders of magnitude). Those trends indicate that the structural modifications, with the substitution of two methylene groups by two ethyleneoxy groups provide ways to increment the basicity of the resulting macrocycles. This can be generated either by the participation of the oxygen atoms, *via* hydrogen bonding, in the protonation process, or by providing additional conformational flexibility so that electrostatic repulsions are better accommodated. This increase in basicity is an interesting feature for the use of those compounds as receptors for anions as is the case of nucleotides.

As in other cases, the basicity of these oxaaza macrocycles is directly related to the length of the aliphatic spacers linking the nitrogen atoms, the larger spacers giving rise always to higher protonation constants. This is also reflected in the prevalence of different protonated species at a given pH value. Thus, for instance, at pH values of biological relevance (pH ≈ 7), H_4**L** and H_3**L** are the dominant species in solution for **Re343**,‡ while for **Re222** and **Re323** no tetraprotonated species can be detected and a mixture of H_3**L** and H_2**L** species is present at this pH (see Fig. 2 and ESI for distribution diagrams†). Similar trends are observed at more acidic pH values. At pH = 4, only H_4**L** species are present in solution for **Re343** and **Re323**. However, for **Re222**, H_3**L** is the major species at this pH while H_4**L** is present only to a very minor extent.

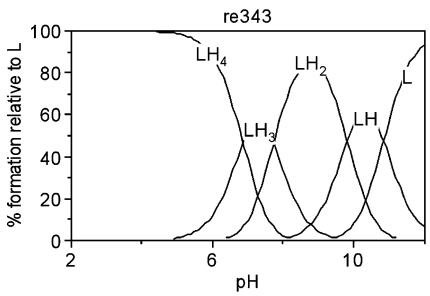

Fig. 2 Distribution diagram for the protonated species of **Re343**. For other ligands, see ESI.†

NMR spectroscopy

In order to gain further insight into the nature of the different species involved, we recorded the NMR spectra of the ligands at different pH values. All the assignments were made on the

‡ Throughout the text, charges have been omitted for clarity in H_x**L** species.

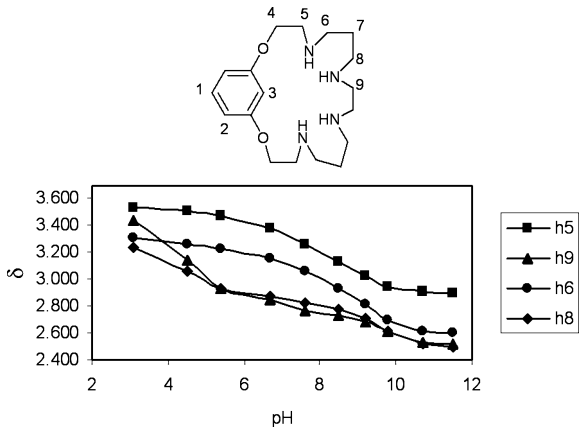

Fig. 3 Variation of the δ values with pH for the protons in the aliphatic region for compound **Re323**.

basis of 2D ^{1}H–^{1}H and ^{1}H–^{13}C correlation experiments. Thus, for instance, Fig. 3 shows the variation of the signals corresponding to the aliphatic protons of the ^{1}H NMR spectra obtained for **Re323** at different pH values.

According to the distribution diagram, for this compound $H_3\mathbf{L}$ is the predominant species in the pH range 4–7 (see Fig. S1 in the ESI†). As can be seen in the figure, only protons 8 and 9 show significant changes below this pH range, which suggests that the first deprotonation mainly affects a proton located at one of the central nitrogen atoms. Diprotonated species are prevalent at pH = 7–9 and the changes in the chemical shifts that accompany their formation mostly affect protons 5 and 6, suggesting that the second deprotonation is preferentially associated with the nitrogen atoms closer to the aromatic subunit. In this case, however, the other possible diprotonated species seem to be also present, even if to a minor extent. Finally, the monoprotonated species only exist in a much reduced pH range (9–10) and their formation is accompanied by changes in the chemical shifts of all the aliphatic protons, indicating the coexistence of the two possible species. The overall protonation scheme for this compound is depicted in Scheme 1.

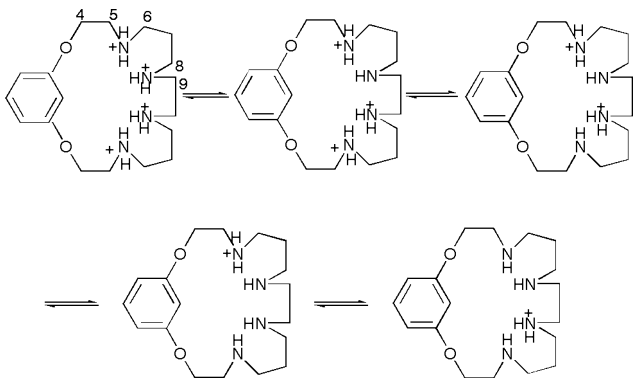

Scheme 1 Protonation sequence for **Re323** according to NMR data.

On the other hand, the study of the aromatic region of the ^{1}H NMR spectra for this compound reveals that only the H atom *ortho* to both ether moieties (H1) is clearly affected by the protonation process (see Fig. 4). The singlet signal corresponding to this proton experiences significant downfield shifts upon

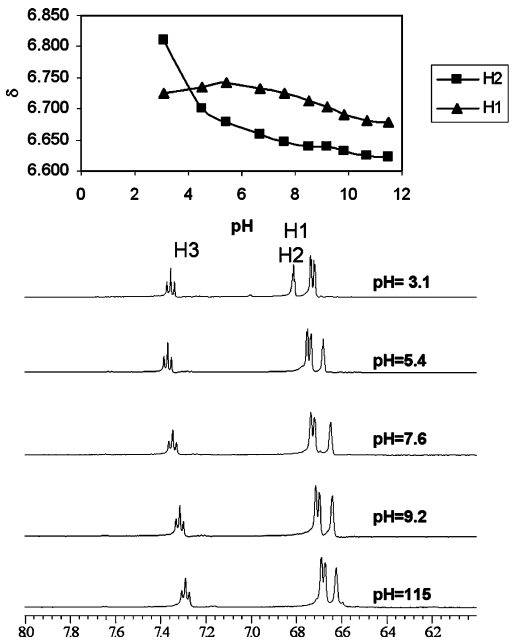

Fig. 4 Variations observed in the aromatic region of the ^{1}H NMR spectra for **Re323**.

protonation ($\Delta\delta \approx 0.2$ ppm). These δ shifts in H1 can be attributed to field effects due to conformational changes associated with the participation of the lone pairs of the oxygens in hydrogen bonding or dipolar interactions (see Scheme 2).

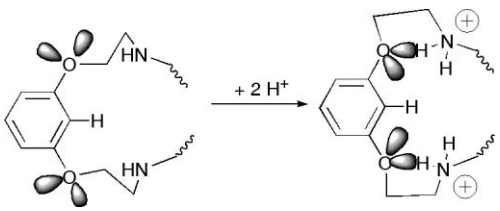

Scheme 2

Similar analyses were carried out for the other ligands (see ESI for the suggested average protonation sequences and NMR data†). Thus, for **Re33** all the aliphatic protons show similar variations in their chemical shifts throughout the whole pH range, revealing that the two possible species coexist for both $H_2\mathbf{L}$ and $H_1\mathbf{L}$. For the macrocycle **Re222**, containing three ethylenic spacers, triprotonated species are prevalent over a broad pH range (4–8). The loss of the first proton from $H_4\mathbf{L}$ is accompanied by a variation in the chemical shifts of the protons in the vicinity of the central nitrogen atoms, clearly showing that the first deprotonation takes places preferentially at this site. Nevertheless, for the second and third deprotonation steps, variations in the δ values affect all protons located next to both kinds of nitrogen atoms. Accordingly, it can be deduced that again the two alternative structures coexist for the mono and diprotonated species. Finally, for **Re343** the first deprotonation takes place at pH 6–7 and the NMR data indicate that the nitrogen atoms located closer to the aromatic ring are the ones essentially involved in this step. When the formation of the diprotonated species, which is prevalent for the pH range 8–10, takes place, NMR data suggest that the species with the protons located at the two central nitrogen atoms is mostly present. In the

same way, the monoprotonated species seems to have the proton mainly located at one of the central nitrogen atoms.

Molecular modelling

In order to better rationalize the role played by the ethyleneoxyphenyl moieties on the acid base behaviour of those compounds, we carried out an extensive set of molecular modelling calculations on the different possible protonated species for all the macrocyclic compounds considered. For that purpose, we made molecular mechanics calculations using the MACROMODEL 7.0 software package.[8] According to our previous experience with related systems,[9] all calculations were made with the AMBER* force field as implemented in the former package.[10] The simulation of water as the solvent was carried out using the GB/SA method.[11] For each protonated species, a conformational search was carried out through the variation of the torsional angles according to the Monte Carlo method, so that for each species, 1000 structures obtained by the automatic variation of the angles were minimized. Fig. 5 shows the minimum energy conformers obtained for the protonated species of the four macrocycles. In those structures, hydrogen bonds are depicted using a dashed black line, while favourable electrostatic interactions are shown by a dotted grey line. It can be seen that hydrogen bonding patterns follow the usual trends for this kind of structure,[12] but only favourable electrostatic interactions can be detected between the oxygen atoms and the adjacent ammonium groups. This could have an effect on the stabilization of highly protonated species as it has been shown to happen in some oxaazamacrocycles.[13] Such an interaction could help to explain the large constant obtained for the third protonation step of **Re222**. Although in order to minimize electrostatic repulsion third protonation yields an expansion of the cycle, only in this case all the possible favourable electrostatic interactions between electron pairs of donor atoms and ammonium are preserved (see dotted lines in Fig. 5).

On the other hand, molecular dynamics calculations using also the AMBER* force field and the GB/SA method reveal that, as in other cases, the protonated species present a much higher degree of preorganization. This is clearly illustrated in Fig. 6 that shows

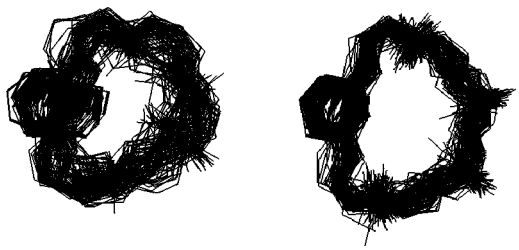

Fig. 6 Superimposition of 100 structures found during MD simulation of **L** and H_4**L** species for **Re323**.

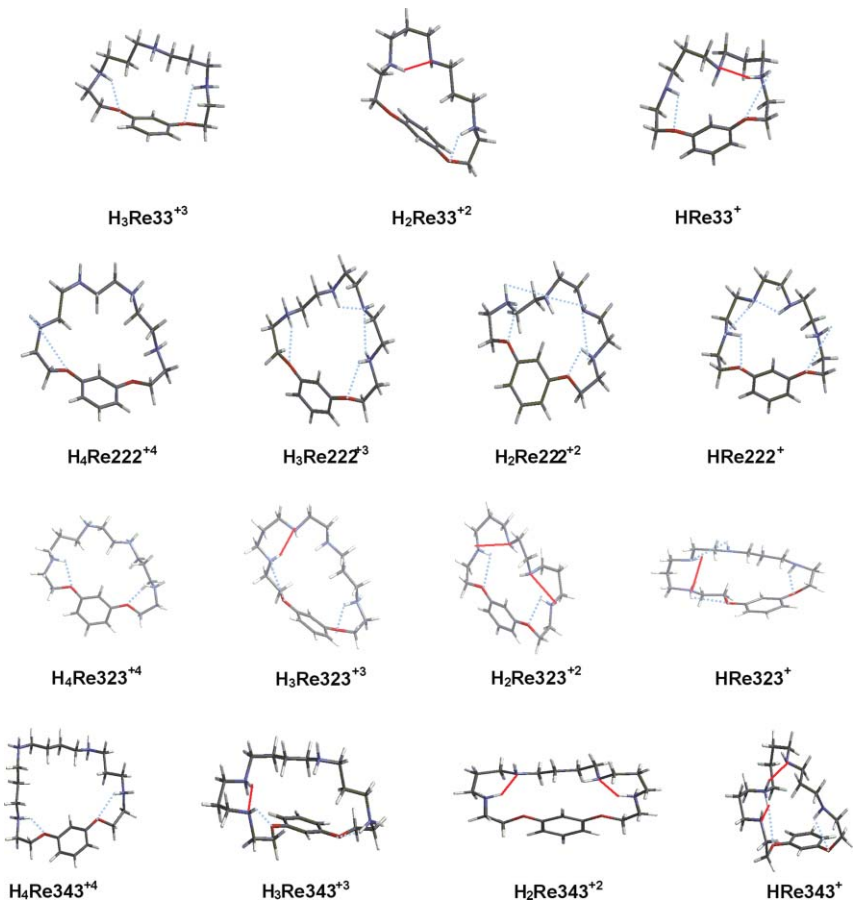

Fig. 5 Minimum energy conformers for protonated species of oxaaza cyclophanes. Dotted blue lines are ammonium–lone pair contacts. Solid red lines represent hydrogen bonds.

a superimposition of 100 structures found during the simulation for the **L** and H_4**L** species for **Re323**.

Molecular spectroscopy

UV–VIS measurements also confirm that oxygen atoms do play a role in the protonation process. This is exemplified for **Re323** in Fig. 7. As can be seen in the figure, an increase in the pH value of an aqueous solution of this macrocycle is accompanied by a bathochromic shift for the band characteristic of the aromatic subunit. This can be easily monitored (see inset in the figure) by recording the variation with pH of the absorbance at 300 nm. The observed change is minor for the pH range 2–7, but a steady increase occurs for higher pH values. This can be associated with the fact that at acidic pH values, where H_3**L** and H_4**L** predominate, the nitrogen atoms adjacent to the ether moieties are protonated at a higher extent and a strong interaction of the oxygen atoms with those ammonium groups is present as suggested by molecular modelling. Thus, the increase in absorption above pH 7 reflects the progressive deprotonation of the lateral nitrogen atoms, modifying the location of the lone pairs of the oxygen atoms in order to maximise the conjugation with the aromatic system (see Scheme 2). Analysis of fluorescence spectra provides a similar outcome.

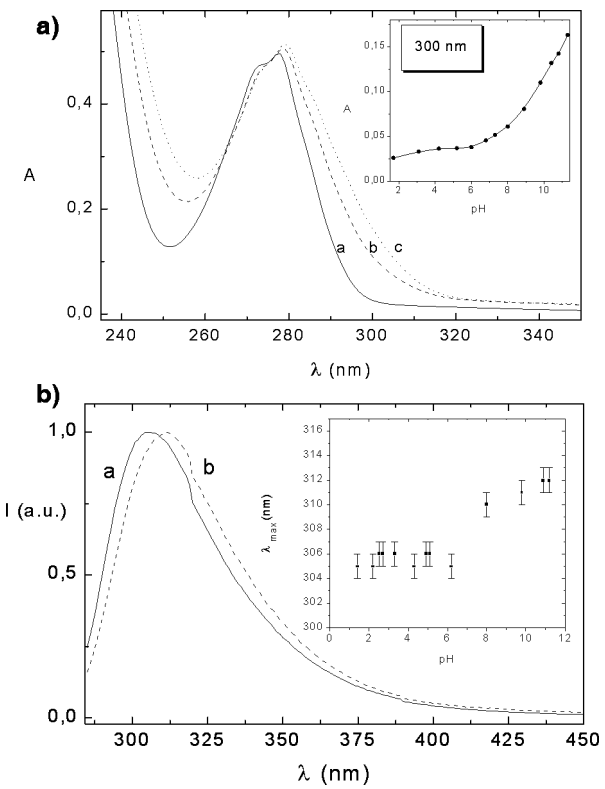

Fig. 7 (a) Absorption spectra for **Re323** at different pH values (a: 1.7; b: 9.8; c: 11.3). The inset shows the variation of the absorbance at 300 nm as a function of pH. (b) Fluorescence spectra (irradiation at 275 nm) for **Re323** at different pH values (a: 2.2; b: 11.2). The inset shows the variation of the position of the fluorescence maximum as a function of pH.

Interaction with nucleotides

Potentiometric measurements. pH titrations show that all receptors significantly interact with nucleotides, in particular **ATP** and **ADP** (see Tables 2 and 3). The nucleotide : receptor stoichiometry of the adducts detected is always 1 : 1. The extent of protonation of the species formed range from 1 to 6 for the pH range under study (3–10). The values for the stepwise formation constants of the adducts show that **ATP** is always the substrate interacting strongest with all the receptors. On the other hand, receptor **Re343** is the one forming the most stable adducts either with **ATP** or **ADP**.

Table 2 Log *K* values for the association constants obtained for receptors **1–4** and **ATP**, determined at 298.1 K in NaCl 0.15 mol dm^{-3}

Reaction[a]	Re33	Re222	Re323	Re343
L + A + H ⇌ HAL	13.50(5)[b]	14.81(7)	13.38(4)	
L + A + 2H ⇌ H_2AL	22.71(3)	23.92(7)	23.00(2)	25.26(3)
L + A + 3H ⇌ H_3AL	30.21(3)	31.96(6)	31.17(2)	34.52(3)
L + A + 4H ⇌ H_4AL	36.52(3)	38.23(7)	38.13(2)	42.08(4)
L + A + 5H ⇌ H_5AL	40.66(4)	42.92(7)	43.41(3)	48.50(4)
L + A + 6H ⇌ H_6AL	42.93(8)	45.8(1)	47.00(4)	52.57(4)
L + A + 7H ⇌ H_7AL		48.5(2)	49.7(1)	
LH + A ⇌ HAL	3.20	4.59	3.27	
LH_2 + A ⇌ H_2AL	4.12	4.95	3.80	4.6
LH_2 + AH ⇌ H_3AL	4.95			
LH_3 + A ⇌ H_3AL	4.88		4.53	6.13
LH_3 + AH ⇌ H_4AL	4.52	5.93	4.82	7.02
LH_4 + AH ⇌ H_5AL			5.07	6.57
LH_3 + AH_2 ⇌ H_5AL	4.58	5.51		
LH_3 + AH_3 ⇌ H_6AL	5.58			
LH_4 + AH_2 ⇌ H_6AL		5.3	4.55	6.56

[a] Charges omitted. [b] Values in parentheses are standard deviations in the last significant figure.

Table 3 Log *K* values for the association constants obtained for receptors **1–4** and **ADP**, determined at 298.1 K in NaCl 0.15 mol dm^{-3}

Reaction[a]	Re33	Re222	Re323	Re343
L + A + H ⇌ HAL		13.1(1)	12.48(5)	13.3(2)
L + A + 2H ⇌ H_2AL	21.17(2)[b]	22.18(8)	22.03(2)	23.66(5)
L + A + 3H ⇌ H_3AL	28.37(2)	30.01(7)	30.03(2)	32.11(4)
L + A + 4H ⇌ H_4AL		35.82(8)	36.79(2)	39.30(4)
L + A + 5H ⇌ H_5AL		40.37(7)	41.75(2)	45.33(5)
L + A + 6H ⇌ H_6AL			45.34(2)	48.93(9)
LH + A ⇌ HAL		2.88	2.37	2.47
LH_2 + A ⇌ H_2AL	2.58	3.21	2.83	3.00
LH_2 + AH ⇌ H_3AL	3.22	4.88		
LH_3 + A ⇌ H_3AL	3.03	3.38	3.38	3.72
LH_3 + AH ⇌ H_4AL		3.03	3.99	4.36
LH_3 + AH_2 ⇌ H_5AL	3.68			
LH_4 + AH ⇌ H_5AL			3.96	3.52
LH_4 + AH_2 ⇌ H_6AL			3.60	3.0

[a] Charges omitted. [b] Values in parentheses are standard deviations in the last significant figure.

Taking into consideration that both the ligands and the nucleotides can participate in several overlapped protonation equilibria, care has to be taken in order to decide the equilibria representative of the formation of a given nucleotide–receptor adduct. Some years ago, our group proposed a method, based on the use of the classical conditional effective stability constants, to overcome those difficulties in the analysis of this kind of system.[14]

At a given pH value, for each ligand **L**, a conditional stability constant can be defined according to the equation:

$$K_{ef} = \frac{\Sigma[LAH_j]}{\Sigma[LH_j]\Sigma[AG_j]} \quad (1)$$

These conditional stability constants are very useful when, at a given pH value, different equilibria can be considered for the formation of the same species. Thus, for instance, at pH = 7 the logarithm of K_{ef} for the interaction of **Re323** with **ATP** is 4.49. At this pH value, H_3**LA** and H_4**LA** species are present and their formation can be described in terms of two different equilibria:

$$H_4\mathbf{L}^{4+} + \mathbf{A}_4^{4-} \leftrightarrow H_4\mathbf{LA} \log K = 6.09$$

$$H_3\mathbf{L}^{3+} + H\mathbf{A}^{3-} \leftrightarrow H_4\mathbf{LA} \log K = 4.82$$

Taking into consideration the individual stability constants for both equilibria and the value of the conditional stability constant for that pH (4.49), it is clear that the participation of the first equilibrium can be discarded.

The use of the conditional stability constants also allows for a simple graphical comparison of the selectivity trends in those systems. This is illustrated in Fig. 8 for the interaction of the different receptors with **ATP** over the whole pH range. The representation of the conditional stability constants at the different pH values allows us to observe that **Re343** is the receptor providing the most intense interaction with **ATP** except for the more basic pH region. This could be ascribed to the higher basicity of this compound (see Table 1) that favours the presence of more highly charged species for a given pH value. Nevertheless, other factors, such as the preorganization of the receptor and the host–guest complementarity must be also considered. Thus, when comparing **Re323** and **Re222**, it is the smaller macrocycle, and accordingly the less basic, the one interacting more strongly with **ATP**. In this regard, **Re323** behaves in a similar way to the smallest macrocycle **Re33**.

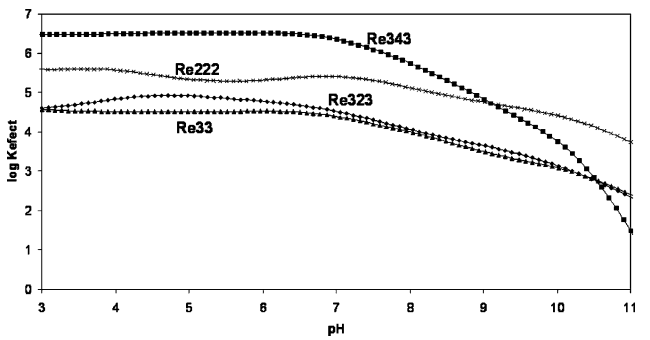

Fig. 8 Plots of the conditional stability constants *vs.* pH for the interaction with **ATP** of oxaaza macrocycles.

As a matter of fact, **Re343** is able to interact with **ATP** stronger than other related polyaza cyclophanes of significantly larger size such as ***m*-B33233**. Fig. 9 shows how **Re343** presents conditional stability constants that are up to 3.5 orders or magnitude higher than those for ***m*-B33233**.

In general, it seems that the presence of the resorcinol derived subunit provides, according to the basic principles in the design of these oxaaza macrocycles, some favourable features for the interaction with **ATP**, and the values of the conditional stability constants determined for them are higher than those found for polyaza cyclophane receptors having the same number and arrangement of nitrogen atoms. This can be seen in Fig. 10 for the case of **Re323**. The conditional stability constants for this receptor are at least one order of magnitude higher, for the entire pH range,

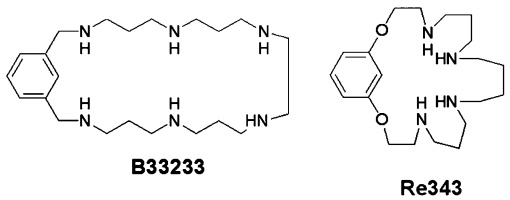

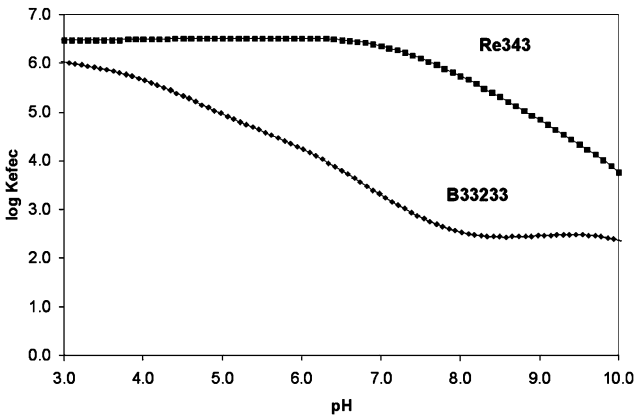

Fig. 9 Plots of the conditional stability constants *vs.* pH for the interaction with **ATP** of **Re343** and **B33233**.

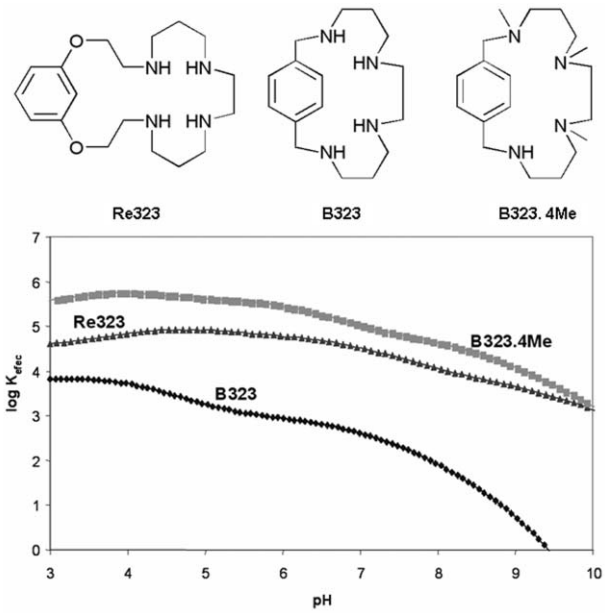

Fig. 10 Plots of the conditional stability constants *vs.* pH for the interaction with **ATP** of **Re323**, **B323** and **B323·4Me**.

than the ones corresponding to **B323**. Only when the ligand **B323** is *N*-alkylated (**B323·4Me**) do the constants become comparable.[3]

When considering the interaction with the different nucleotides, **ATP**, **AMP**, **ADP**, the general trends are similar to those obtained with related systems and the strength of the interaction follows the order **ATP** > **ADP** > **AMP**.[1–4] In our case, the low values for the association constants of **AMP** with the different receptors precluded their accurate determination except for the more basic ligand **Re343** (see Table 4).

Table 4 Log K values for the association constants obtained for receptors **Re343** and **AMP**, determined at 298.1 K in NaCl 0.15 mol dm^{-3}

Reaction[a]	**Re343**
$L + A + H \rightleftharpoons HAL$	14.30(6)
$L + A + 2H \rightleftharpoons H_2AL$	24.29(5)
$L + A + 3H \rightleftharpoons H_3AL$	32.39(4)
$L + A + 4H \rightleftharpoons H_4AL$	39.37(4)
$L + A + 5H \rightleftharpoons H_5AL$	45.16(4)
$LH + A \rightleftharpoons HAL$	3.46
$LH_2 + A \rightleftharpoons H_2AL$	3.63
$LH_2 + AH \rightleftharpoons H_3AL$	5.41
$LH_3 + A \rightleftharpoons H_3AL$	4.0
$LH_4 + A \rightleftharpoons H_4AL$	4.11
$LH_4 + AH \rightleftharpoons H_5AL$	3.58

[a] Charges omitted. [b] Values in parentheses are standard deviations in the last significant figure.

In the case of **Re343**, Fig. 11 shows how this ligand is able to selectively interact with **ATP** in the presence of **ADP** and **AMP**, the selectivities observed always being above 100 in the acidic pH range (851 at neutral pH). Rather surprisingly, no significant differences are observed between **ADP** and **AMP** in the pH range 4–7. At lower pH values **ADP** interacts more strongly, while **AMP** complexes are predominant (over those of **ADP**) at basic pH values.

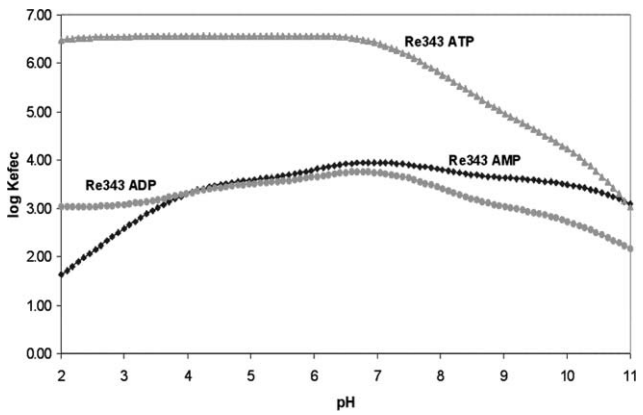

Fig. 11 Plots of the conditional stability constants *vs.* pH for the interaction of **Re343** with **ATP**, **ADP** and **AMP**.

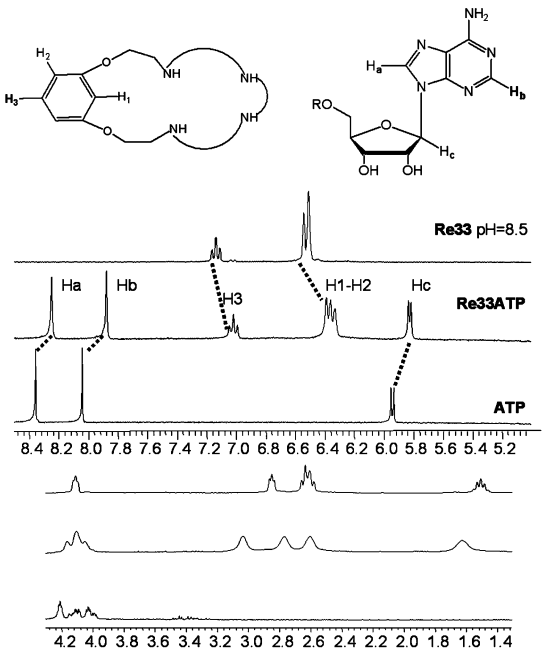

Fig. 12 ^{1}H NMR spectra for the aromatic (upper traces) and aliphatic (lower traces) regions for **Re33**, **ATP** and an equimolecular mixture of both at pH = 8.5.

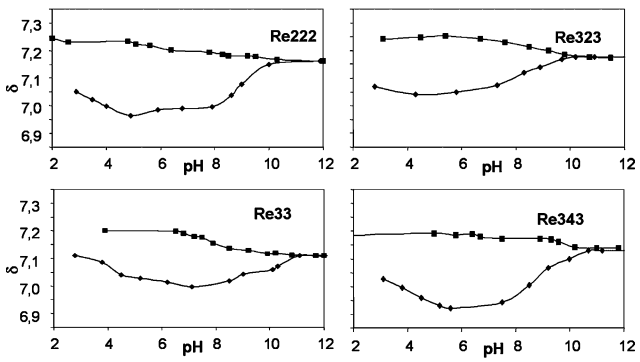

Fig. 13 Chemical shifts observed, at different pH values, for the aromatic proton H_3 in macrocylces **Re33**, **Re323**, **Re323** and **Re343** upon interaction with **ATP**.

NMR measurements

Additional information on the nature of complex species formed was obtained through the use of NMR spectroscopy. As an example, Fig. 12 shows the aromatic (a) and aliphatic (b) regions at pH = 8 of the NMR spectra for free **Re343**, **ATP** and for the corresponding complex species. The spectra show how the formation of the complexes is accompanied by a significant broadening of the signals of both the receptor and the nucleotide. This can be ascribed to the conformational restrictions that take place upon formation of the complex species. On the other hand, the aromatic signals of receptor and substrate experience an upfield shift, which is consistent with the formation of complex structures with stacked aromatic rings.[3]

This is a general behaviour for the different receptors considered in this work. Thus, Fig. 13 shows the variation in the chemical shift observed for the aromatic proton H_3 of the macrocycles **Re33**, **Re323**, **Re323** and **Re343** upon interaction with **ATP** at different pH values. In the same way, Fig. 14 gathers the information about the variation in the chemical shift observed for the aromatic proton H_b of **ATP** under the same conditions (for the atom labelling, see Fig. 12).

As can be seen, shielding of the aromatic signals of both receptor and ATP occurs for the whole pH range for which complex species formation is significant and this shielding is similar for all the receptors considered. Thus, for the system **Re323**–**ATP** at pH = 3, for which the complex species H_6**LA** is predominant, the signal corresponding to H_3 is observed 0.1 ppm shielded relative to that of the free macrocycle at that pH value. For pH values close to 7, where the predominant complex species is H_4**LA**, a maximum shielding of *ca.* 0.2 is observed. For higher pH values, the observed shielding decreases to essentially disappear after reaching

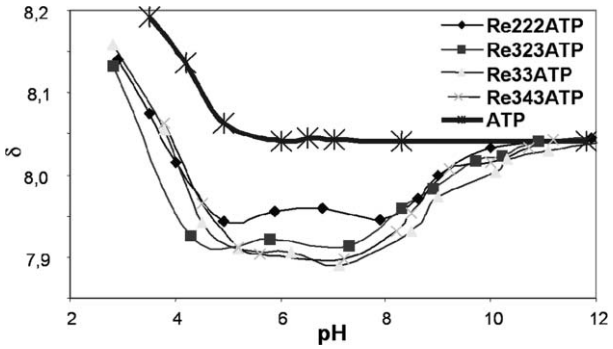

Fig. 14 Chemical shifts observed, at different pH values, for the aromatic proton H_b of **ATP** upon interaction with macrocylces **Re33**, **Re323**, **Re323** and **Re343**.

pH = 10. Very similar trends can be described for the H_b proton of the adenine fragment.

The formation of complex structures presenting some degree of stacking for the aromatic rings occurs for the three nucleotides studied. This is illustrated in Fig. 15 that shows the variation of the chemical shift for the H_1 proton of the free macrocycle **Re343** at different pH values and for the complex species formed with **ATP**, **ADP** and **AMP**. It can be observed how the shielding is essentially the same for **ATP** and **ADP** but is clearly reduced for **AMP**. This suggests that for **AMP**, stacking interactions can be less efficient.

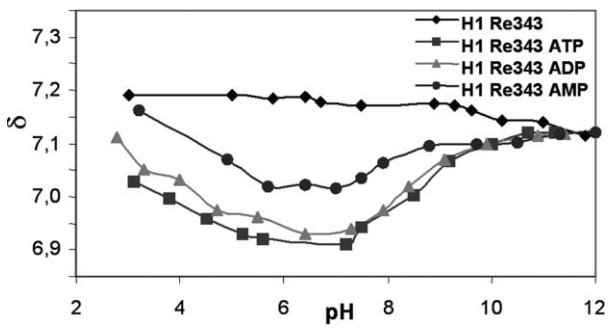

Fig. 15 Chemical shifts observed, at different pH values, for the aromatic proton H_1 of **Re343** upon interaction with **ATP**, **ADP** and **AMP**.

Complementary information can be obtained through the use of ^{31}P NMR spectroscopy. In this regard, Fig. 16 displays the ^{31}P NMR spectra of **ATP** free and complexed with **Re323** at pH = 7. A significant downfield shift, accompanied by a broadening of the signals, is observed for the peaks corresponding to P_γ and P_β, the effects on P_γ being larger. On the contrary, the signal for P_α remains essentially unchanged. The changes in the shift of the signals for P_γ and P_β reflect the change in the extent of protonation of **ATP** and the conformational changes required to optimize the electrostatic interaction. This occurs when **ATP** increases its negative charge density and the receptor increases its protonation degree (as can be seen at the bottom traces in Fig. 12, complexation is always accompanied by an increase in the protonation degree of the nitrogen atoms that is reflected in a downfield shift of the methylene groups close to them).

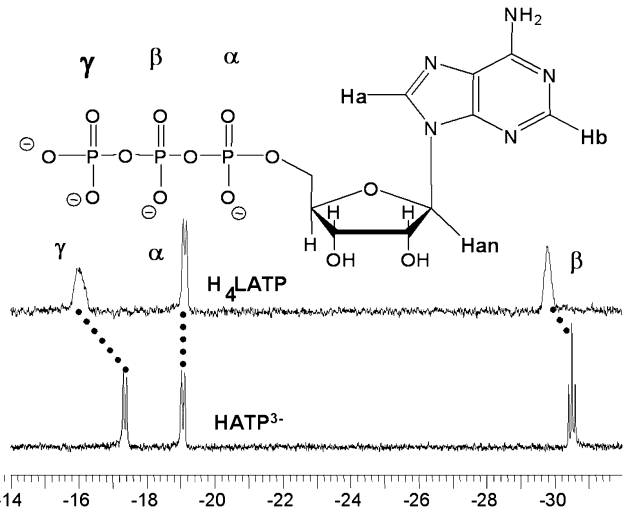

Fig. 16 ^{31}P NMR spectra of **ATP** free and complexed with **Re323** at pH = 7.

Molecular modelling

Molecular dynamics simulations and molecular mechanics calculations for the different complexes were carried out in a similar way to that previously reported for protonated receptors. The conformational search for each individual complex species always provided minimum energy conformers containing stacked geometries for the aromatic rings of the macrocycle and the nucleotide. The minimum energy conformer calculated for the system H_4**Re343**·H**ATP** (the predominant species at pH around 5) is depicted in Fig. 17 and shows an excellent complementarity between **ATP** and the macrocycle. In this regard, optimization of the π–π and electrostatic interactions takes place without introducing any significant conformational stress in the components. The situation is, however, different when the interaction of **ATP** with the smaller macrocycles is considered or for the interaction of **Re343** with **ADP** or with **AMP**, which could justify the lower stabilities observed for the corresponding complex species.

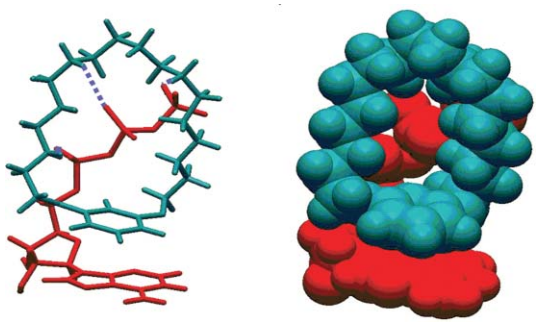

Fig. 17 Minimum energy structure for H_4**Re343**$^{4+}$–**HATP**$^{3-}$.

Molecular dynamics studies allow evaluation of the relative receptor–substrate mobility of the corresponding complex species. Fig. 18 shows the superimposition of the structures found during a 5 ns molecular dynamics simulation for the systems **Re343**·**ATP** and **Re343**·**AMP**. It can be seen how the first complex species, the one being more stable, is much more rigid than the second one as a consequence of the better complementarity shown by the two

Fig. 18 Superimposition of 50 structures found during the MD simulation of **Re343**·**ATP** and **Re343**·**AMP** species.

components. It is noteworthy that stacking of the aromatic rings is maintained throughout the whole simulation process.

Molecular spectroscopy

UV–Visible measurements were carried out in order to detect any potential electronic interaction of the aromatic rings. No such interactions could be, however, detected, but a significant increase in the absorption above 300 nm was observed in some cases. This phenomenon is associated with the formation of turbidity in the samples that is visible to the naked eye in the pH range 4–6. As can be seen in Fig. 19 for **Re323**, this is associated with the formation of 1 : 1 complex species that present a low solubility in aqueous solutions. An analysis of the whole pH range reveals, as shown in Fig. 20, this turbidity can be ascribed to the presence of the neutral species H_4**LA** or the monocation H_5**LA**. The low solubility of these species with low charge could be potentially used in purification processes for nucleotides.

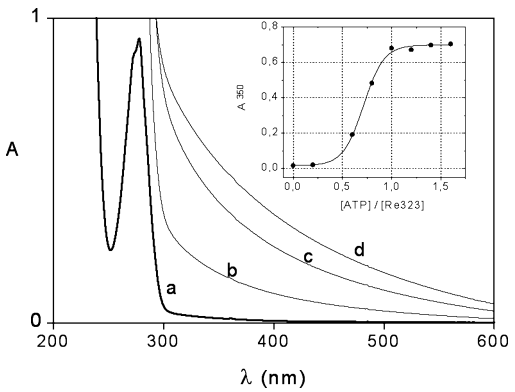

Fig. 19 UV–VIS spectra for **Re323** (5e-4M) in water at pH = 5.0 upon addition of **ATP**: (a) 0 mol dm^{-3}**ATP**; (b) 3e-4 mol dm^{-3}**ATP**; (c) 4e-4 mol dm^{-3}**ATP**; (d) 5e-4 mol dm^{-3} **ATP**. Inset: variation of the absorbance at 350 nm as a function of the concentration of **ATP**.

Conclusions

The presence of oxygen donor atoms and electron-rich aromatic rings in oxaaza cyclophanes derived from resorcinol provides some interesting properties to the resulting abiotic receptors. In general, the overall basicity of the present macrocycles is higher than that observed for related systems not containing the ethyleneoxy subunits. This is particularly significant for **Re222** having an overall basicity constant four orders of magnitude higher than that of **B222**. According to our results, the presence of the ethyleneoxy

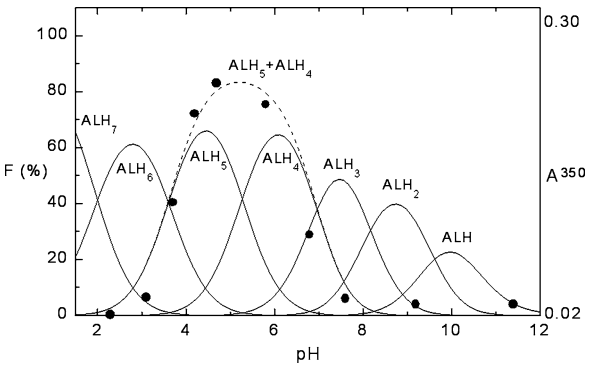

Fig. 20 Distribution diagram for **Re323** (5e-4 mol dm^{-3}) + **ATP** (5e-4 mol dm^{-3}) species. The values of the absorbance at 350 nm at different pH values are given by black dots (●). The dotted line represents the sum of H_5**L**A and H_4**L**A species.

subunits can contribute to increase the conformational flexibility of the system (and favouring the release of charge–charge interactions) and through the participation of oxygen atoms in the stabilization of protonated species.

All receptors interact significantly with nucleotides to form 1 : 1 adducts in aqueous solution. In all cases, **ATP** is the nucleotide interacting the most strongly. From the different macrocycles, **Re343** is the one forming the most stable adducts either with **ATP** or **ADP**. As a matter of fact, **Re343** is able to interact with **ATP** stronger than other related polyaza cyclophanes of significantly larger size such as **m-B33233** having up to six nitrogen atoms in the macrocyclic structure. In this regard, only *N*-methylated polyaza cyclophanes seem to behave in a similar way. According to the basic features for the design of this family of receptors, the presence of an electron-rich aromatic ring seems to clearly contribute to this behaviour. NMR data are consistent with the formation of complex structures with stacked aromatic rings. This phenomenon is much weaker for adducts formed with **AMP** which reveals a worse structural complementarity in this case, as has been confirmed by molecular modelling studies.

Finally, UV–visible experiments reveal that formation of complex species of low charge, as is the case of H_4**LA** (neutral) or H_5**LA** (monocation) species for **Re323**, is accompanied by a marked decrease in solubility. This opens the way for developing new protocols for nucleotide purification.

Experimental

All the oxaaza cyclophanes were obtained as previously described.[5]

EMF measurements

The potentiometric titrations were carried out at 298.1 ± 0.1 K in $NaClO_4$ 0.15 mol dm^{-3}. The experimental procedure used (burette, potentiometer, cell, stirrer, microcomputer, *etc.*) was the same as one that has been fully described elsewhere.[15] The acquisition of the emf data was performed with the computer program PASAT.[16] The reference electrode was an Ag/AgCl electrode in saturated KCl solution. The glass electrode was calibrated as an hydrogen-ion concentration probe by titration of previously standardized amounts of HCl with CO_2-free NaOH solutions and determining

the equivalent point by Gran's method,[17] which gives the standard potential, $E^{0\prime}$, and the ionic product of water ($pKw = 13.73(1)$). The concentrations of the different metal ions employed were determined gravimetrically by standard methods.

The computer program HYPERQUAD,[18] was used to calculate the protonation and stability constants.

NMR measurements

The ^{1}H and ^{13}C spectra were recorded on a Varian INOVA 500 spectrometer operating at 500 MHz for ^{1}H and 125.75 MHz for ^{13}C. The NMR experiments involving ^{31}P were recorded on a Varian Unity 300 spectrometer equipped with a switchable probe.

Molecular modelling

For the molecular modelling studies, the Macromodel 7.0 software package was used.[8] The simulation of water was carried out using the GB/SA method.[11] For each studied species, the conformational search was carried out through variation of the torsional angles according to the Monte Carlo method: 1000 structures were obtained and minimized for each case.

Acknowledgements

This work was funded by the MCYT and the Fundació Bancaixa-UJI (projects BQU2003-09215, CTQ2006-15672 and P1 1B2004-38). We also thank Dr F. Galindo for his help with UV–visible and fluorescence studies.

Notes and references

1 For general reviews on this subject see: *Supramolecular Chemistry of Anions*, ed. A. Bianchi, E. García-España and K. Bowman-James, Wiley-VCH, New York, 1997; S. Auki and E. Kimura, *Chem. Rev.*, 2004, **104**, 769–787; J. L. Sessler and J. Jayawickramarajah, *Chem. Commun.*, 2005, 1939–1949; S. Sivakova and S. J. Rowan, *Chem. Soc. Rev.*, 2005, **34**, 9–21; E. García-España, P. Díaz, J. M. Llinares and A. Bianchi, *Coord. Chem. Rev.*, 2006, **250**, 2952–2986.

2 M. W. Hosseini, J. M. Lehn, L. Maggiora, K. B. Mertes and M. P. Mertes, *J. Am. Chem. Soc.*, 1987, **109**, 537–544; M. W. Hosseini, J. M. Lehn, K. C. Jones, K. E. Plute, K. B. Mertes and M. P. Mertes, *J. Am. Chem. Soc.*, 1989, **111**, 6330–6335; P. Cudic, M. Zinic, V. Tomisic, V. Simeon, J. P. Vigneron and J.-M. Lehn, *J. Chem. Soc., Chem. Commun.*, 1995, 1073–1075; M. Onda, K. Yoshihara, H. Koyano, K. Ariga and T. Kunitake, *J. Am. Chem. Soc.*, 1996, **118**, 8524–8530; C. Bazzicalupi, A. Beconcini, A. Bencini, V. Fusi, C. Giorgi, A. Masotti and B. Valtancoli, *J. Chem. Soc., Perkin Trans. 2*, 1999, 1675–1682; S. Aoki and E. Kimura, *J. Am. Chem. Soc.*, 2000, **122**, 4542–4548; M. Sirish and H.-J. Schneider, *J. Am. Chem. Soc.*, 2000, **122**, 5881–5882; S. E. Scheider, S. N. O'Neil and E. V. Anslyn, *J. Am. Chem. Soc.*, 2000, **122**, 542–543; M. E. Padilla-Tosta, J. M. Lloris, R. Martínez-Mañez, T. Pardo, F. Sancenón, J. Soto and M. D. Marcos, *Eur. J. Inorg. Chem.*, 2001, 1221–1226; Y. H. Guo, Q. C. Ge, H. Lin and H. K. Lin, *Polyhedron*, 2002, **21**, 1005–1015; S. R. Zhu, C. Bazzicalupi, S. Biagini, A. Bencini, E. Faggi, C. Giorgi, I. Matera and B. Valtancoli, *Chem. Commun.*, 2005, 4087–4089; Y. Hisamatsu, K. Hasada, F. Amano, Y. Tsubota, Y. Wasada-Tsutsui, N. Shirai, S. Ikeda and K. Odashima, *Chem.–Eur. J.*, 2006, **12**, 7773–7741.

3 J. A. Aguilar, E. García-España, J. A. Guerrero, S. V. Luis, J. M. Llinares, J. A. Ramírez and C. Soriano, *J. Chem. Soc., Chem. Commun.*, 1995, 2237–2239; J. A. Aguilar, E. García-España, J. A. Guerrero, S. V. Luis, J. M. Llinares, J. A. Ramírez and C. Soriano, *Inorg. Chim. Acta*, 1996, **245**, 287–294; M. I. Burguete, P. Diaz, E. García-España, S. V. Luis, J. F. Miravet, M. Querol and J. A. Ramírez, *Chem. Commun.*, 1999, 649–650; J. A. Aguilar, A. B. Descalzo, P. Diaz, V. Fusi, E. García-España, J. A. Ramírez, P. Romano and C. Soriano, *J. Chem. Soc., Perkin Trans. 2*, 2000, 1187–1192; J. A. Aguilar, B. Celda, V. Fusi, E. García-España, S. V. Luis, M. C. Martínez, J. A. Ramírez, C. Soriano and R. Tejero, *J. Chem. Soc., Perkin Trans. 2*, 2000, 1323–1328; M. T. Albelda, J. C. Frías, E. García-España and S. V. Luis, *Org. Biomol. Chem.*, 2004, **2**, 816–820.

4 M. W. Hosseini, A. J. Blacker and J.-M. Lehn, *J. Am. Chem. Soc.*, 1990, **112**, 3896–3904; Y. Kato, M. M. Conn and J. Rebek, *Proc. Natl. Acad. Sci. U. S. A.*, 1995, **92**, 1208–1212; S. M. Butterfield, M. M. Sweeney and M. L. Waters, *J. Org. Chem.*, 2005, **70**, 1105–1114.

5 M. I. Burguete, L. López-Diago, E. García-España, F. Galindo, S. V. Luis, J. F. Miravet and D. Sroczynski, *J. Org. Chem.*, 2003, **68**, 10169–10171.

6 A. Bianchi, B. Escuder, E. García-España, S. V. Luis, V. Marcelino, J. F. Miravet and J. A. Ramirez, *J. Chem. Soc., Perkin Trans. 2*, 1994, 1253–1259.

7 A. Bencini, A. Bianchi, E. García-España, M. Micheloni and J. A. Ramírez, *Coord. Chem. Rev.*, 1999, **188**, 97–156; C. Frassinetti, L. Alderighi, P. Gans, A. Sabatini, A. Vacca and S. Ghelli, *Anal. Bioanal. Chem.*, 2003, **376**, 1041–1052; J. E. Sarneski, H. L. Surprenant, F. K. Molen and C. N. Reilley, *Anal. Chem.*, 1975, **47**, 2116–2124; D. N. Hague and A. D. Moreton, *J. Chem. Soc., Perkin Trans. 2*, 1994, 265–270.

8 F. Mohamadi, N. G. J. Richards, W. C. Guida, R. Liskamp, M. Lipton, C. Caufield, G. Cheng, T. Hendrickson and W. C. Still, *J. Comput. Chem.*, 1990, **11**, 440–467.

9 B. Altava, A. Bianchi, C. Bazzicalupi, M. I. Burguete, E. García-España, S. V. Luis and J. F. Miravet, *Supramol. Chem.*, 1997, **8**, 287–299; M. I. Burguete, B. Escuder, E. García-España, L. López, S. V. Luis, J. F. Miravet and M. Querol, *Tetrahedron Lett.*, 2002, **43**, 1817–1819; J. Becerril, M. Bolte, M. I. Burguete, F. Galindo, E. García-España, S. V. Luis and J. F. Miravet, *J. Am. Chem. Soc.*, 2003, **125**, 6677–6686.

10 S. J. Weiner, P. A. Kollman, D. Case, V. C. Singh, C. Ghio, G. Alagona, S. Profeta and P. Weiner, *J. Am. Chem. Soc.*, 1984, **106**, 765–784.

11 W. C. Still, A. Tempczyk, R. C. Hawley and T. Hendrickson, *J. Am. Chem. Soc.*, 1990, **112**, 6127–6129.

12 C. Bazzicalupi, A. Bencini, A. Bianchi, M. Cechi, B. Escuder, V. Fusi, E. García-España, C. Giorgi, S. V. Luis, G. Maccagni, V. Marcelino, P. Paoletti and B. Valtancoli, *J. Am. Chem. Soc.*, 1999, **121**, 6807–6815.

13 M. P. Mertes and K. B. Mertes, *Acc. Chem. Res.*, 1990, **23**, 413–418; V. J. Aran, M. Kumar, J. Molina, L. Lamarque, P. Navarro, E. García-España, J. A. Ramirez, S. V. Luis and B. Escuder, *J. Org. Chem.*, 1999, **64**, 6135–6146; D. K. Chand, H.-J. Schneider, A. Bencini, A. Bianchi, C. Giorgi, S. Ciattini and B. Valtancoli, *Chem.–Eur. J.*, 2000, **6**, 4001–4008; M. Vicente, R. Bastida, C. Lodeiro, A. Macias, A. J. Parola, L. Valencia and S. E. Spey, *Inorg. Chem.*, 2003, **42**, 6768–6779.

14 A. Andrés, J. Aragó, A. Bencini, A. Bianchi, A. Doménech, V. Fusi, E. García-España, P. Paoletti and J. A. Ramírez, *Inorg. Chem.*, 1993, **32**, 3418–3424; A. Bencini, A. Bianchi, M. I. Burguete, P. Dapporto, A. Doménech, E. García-España, S. V. Luis, P. Paoli and J. A. Ramírez, *J. Chem. Soc., Perkin Trans. 2*, 1994, 569–577; M. T. Albelda, M. A. Bernardo, E. García-España, M. L. Godino, S. V. Luis, M. J. Melo, F. Pina and C. Soriano, *J. Chem. Soc., Perkin Trans. 2*, 1999, 2545–2549.

15 E. García-España, M.-J. Ballester, F. Lloret, J.-M. Moratal, J. Faus and A. Bianchi, *J. Chem. Soc., Dalton Trans.*, 1988, 101–104.

16 M. Fontanelli and M. Micheloni, *Proceedings of the Spanish–Italian Congress on Thermodynamic of Metal Complexes*, Diputación de Castellón, Castellón, Spain, 1990.

17 G. Gran, *Analyst*, 1952, **77**, 661–671; F. J. C. Rossotti and H. Rossotti, *J. Chem. Educ.*, 1965, **42**, 375–378.

18 A. Sabatini, P. Gans and A. Vacca, *Coord. Chem. Rev.*, 1992, **120**, 389–405.

